Article

Not peer-reviewed version

A Dynamic Dark Energy Consistent with DESI and DES: Information Dark Energy

Michael Paul Gough *

Posted Date: 27 June 2025

doi: 10.20944/preprints202506.2213.v1

Keywords: Landauer's Principle; Dark Energy; Dark Energy Experiment

 doi:10.20944/preprints202506.2213.v1

Article

A dynamic Dark Energy Consistent with DESI and DES: Information Dark Energy

Michael Paul Gough

School of Engineering and Informatics, University of Sussex, Brighton, BN1 9QT, m.p.gough@sussex.ac.uk

Abstract

Results from both the Dark Energy Spectrograph Instrument and the Dark Energy Survey collaborations are shown to be compatible with a dark energy driven by star formation. The Landauer energy of the information associated with stars, galaxies, galaxy groups, and galaxy clusters provides a dark energy dependent on source temperature, which is in turn related to source mass. Combining this relation with a survey of stellar mass density measurements yields a predicted Information Dark Energy with CPL parameters: ω_0 = -0.76, ω_a = -1.29, reaching a maximum in the redshift range, $0.2<z<0.6$. These characteristics are similar to the dark energy results of the Dark Energy Spectrograph Instrument and the Dark Energy Survey. A comparison is also made between the stellar mass density history required to account for the dark energy measurements against the actual stellar mass density measurement survey. Both approaches are consistent with a phantom Information Dark Energy driven by star and structure formation. This work emphasizes a data driven approach, combining stellar mass density measurements with the recent dark energy results. Information Dark Energy has the potential to resolve many problems of cosmology and should therefore be considered as a candidate for the source of dark energy.

Keywords: Landauer's Principle; Dark Energy; Dark Energy Experiments

1. Introduction

Landauer's principle [1,2] states that each bit of information in a system at temperature, T, has a minimum equivalent energy of k_B T ln 2. We can put this small quantity into perspective by considering the present ~10 zetabytes held worldwide in the cloud/ AI/ data centres. The data storage and networking aspects of these centres already use ~2 % of the total electricity generated worldwide. However, if all the 10 zetabytes in world data centres were to be erased, the total Landauer energy released as heat at ~300K is miniscule by comparison, only ~200 Joules. This is just the amount used by one electric kettle in 1/10 second. Landauer's principle has now been proven experimentally [3-6] and, linking information to thermodynamics, also provides an important solution to the problem of Maxwell's demon [7].

Despite the little impact that Landauer information energy has on our every day lives, it does nevertheless represent a major source of energy within the universe. A "Foundational Principle" proposed by Anton Zeilinger [8] considers the attributes of all particles, at their most fundamental level, correspond to elemental systems. These are effectively simple 1bit, 'yes'/'no', results of experimental inquiry. In a simple universe without star formation, the Landauer equivalent energy of a Zeilinger elemental particle attribute has been shown [9] to be defined exactly the same as the characteristic energy of a cosmological constant [10]. Moreover, the Landauer equivalent energy has been shown to contribute a significant Information Dark Energy, IDE [11-16] to the universe. The total information energy carried by matter, or represented by matter, is at a similar level to the total mc^2 equivalent energy of the 10^{53} kg baryons in the universe (Figure 7 of [16]). Strong contributions are made by stellar heated gas and the intra-cluster gas within galaxy clusters.

The key to identifying the physical source of dark energy is in determining the dark energy density variation over the history of the universe. The latest results of the Dark Energy Spectrograph

 doi:10.20944/preprints202506.2213.v1

Instrument, DESI, [17] and the Dark Energy Survey, DES, [18] provide evidence for a dynamic dark energy, evidence that excludes the previously assumed cosmological constant at a level >3 σ.

A previous IDE publication [16] only compared IDE against the initial data from DESI and DES, whereas the present work applies the updated final published DESI and DES results. Two versions of the relation between temperature and mass of astrophysical objects are applied; one from a survey of galaxy and galaxy cluster measurements, and one derived from the DESI and DES results, assuming the IDE source of dark energy. This work also extends the Stellar Mass Density (SMD) measurements to higher redshifts. We compare the IDE prediction from the SMD measurement survey against the DES and DESI results. We also compare the SMD variation required to explain the DES and DESI measured values against the survey of SMD measurements, assuming an IDE source of dark energy.

2. Information Dark Energy

2.1. Temperature Dependence

The Landauer equivalent energy of each bit in any system is solely dependent on the system's temperature. We find that the temperatures, T, of several astrophysical structures ranging in mass, M, from 0.1 solar mass, $M_\odot$, to $>10^{15}$ $M_\odot$, each follow a similar relation. The results of a large survey of measured galaxy, galaxy group, and galaxy cluster temperatures [19] have been shown, on average, to closely follow the $T \propto M^p$ relation over the range $<10^{12}$ $M_\odot$ to $>10^{15}$ $M_\odot$, illustrated in Figures 1 B & 1C, where p=0.606. In Figure 1 A we see that the temperature of stars, from 10^{-1} $M_\odot$ to 3×10^{1} $M_\odot$ in the seven main sequence spectral classes also follow the same relation with the same power, p. Note that the previous work on IDE [16] simply considered the values p=0.5, and p=1.0. In this work we also extend the survey of stellar mass density, SMD(a), measurements [20-47] used previously to include measurements at universe scale sizes, a<0.2, [48,49] where a is related to redshift, z, by a=1/(1+z).

2.2. CPL ω_0-ω_a Parameters

The time variation of the dark energy density is proportional to $a^{-3(1+\omega)}$, where ω is the dark energy equation of state parameter. Any dynamic form of dark energy requires a time varying value of ω(a). In order to account for a dynamic dark energy most experimental measurements of dark energy have adopted the common CPL [50] parameters: $\omega(a)= \omega_0 + (1-a)\,\omega_a$. As the most recent DES and DESI dark energy results are published in ω_0 - ω_a parameter space, it is convenient to predict the IDE source of dark energy also in terms of ω_0 - ω_a space.

 doi:10.20944/preprints202506.2213.v1

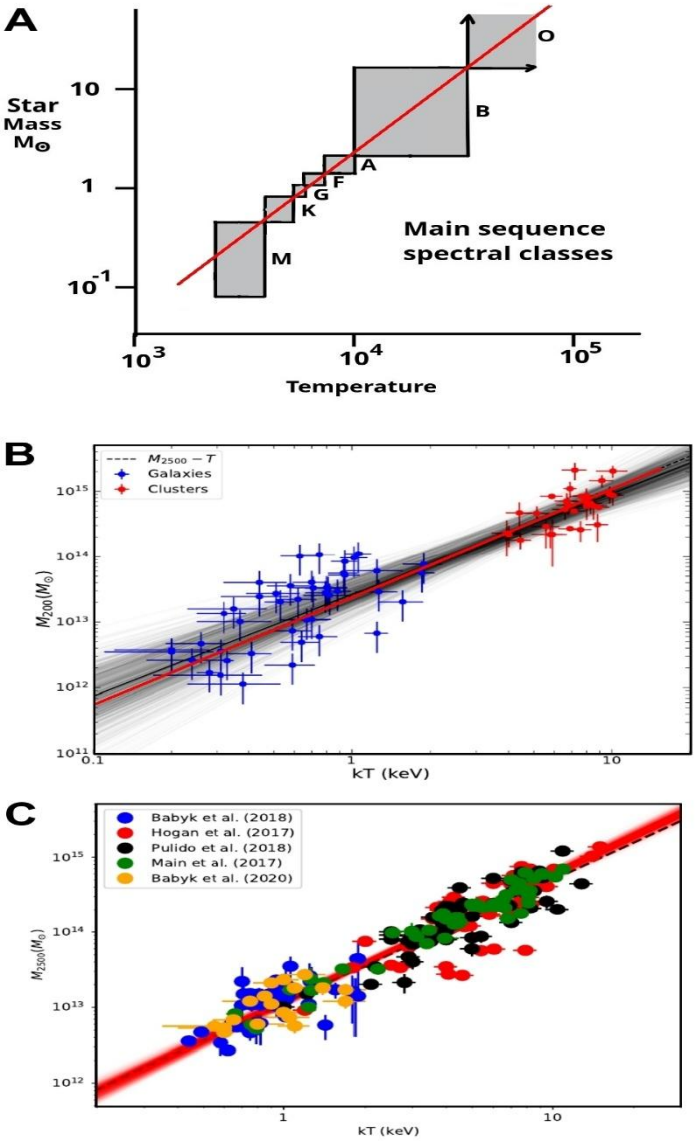

Figure 1. The red lines correspond to temperature proportional to (mass)$^{0.606}$ in all three plots: A, Main sequence star spectral classes; B & C, Galaxies, galaxy groups & galaxy clusters adapted from Figs 2 and 4 of [19].

2.3. Predicted IDE in $\omega_0 - \omega_a$ Space

The Stellar Mass Density is a universe-wide average mass density that changed with time and thus a function of universe scale size: SMD(a). We expect that IDE(a), being proportional to temperature, to vary as IDE(a) $\propto$ SMD(a)^p. At the same time a CPL approximation of IDE energy density variation describes IDE(a) α $a^{-3(1+\omega 0+(1-a)\omega a)}$. Each ω_0 - ω_a combination describes the curve of dark energy density as a function of scale size. Assuming an IDE source of dark energy, the p value transfers that to a SMD(a) curve whose measure of fit to all the measured SMD(a) values [20-49] is given by a R^2 coefficient of determination. R^2 is defined as R^2=1-(RSS/TSS), where RSS is the residual sum of squares, and TSS is the total sum of squares.

There are four DESI and DES dark energy derived ω_0 - ω_a combinations listed in Table 1. DESI combines BAO and CMB with three different sets of supernova measurements, Union3, DESY5, and Pantheon plus, to provide three ω_0 -ω_a values [17]. The most constrained DES ω_0 -ω_a value is listed for a combination of Baryon Acoustic Oscillation, BAO, Supernovae, SN, and Cosmic Microwave Background, CMB, measurements [18].

In Figure 2. the value of R^2 is plotted as a function of p for each of the four experimentally derived DESI and DES ω_0 - ω_a values. The grey line is the average R^2 of the four values. Shown below are the

 doi:10.20944/preprints202506.2213.v1

values of p determined from the temperatures and masses of galaxies and clusters using X-ray and lensing measurements [19]. Figure 2. enabled us to select two data driven values of p to better illustrate the similarity of dark energy history to star formation history. The value p=0.606 was determined directly by actual mass and temperature measurements of galaxy and clusters [19]. The value p=0.461 is determined from the maximum R^2 of the average of all four DES and DESI measurements, assuming IDE. Note that the value p=0.606 also coincides with the maximum of the single DES measurement, and the value p=0.461 coincides with the maximum of the DESI BAO+CMB+Union3 measurement.

Table 1. Published dark energy ω_0 - ω_a CPL values for DES and three DESI combinations of measurement types compared with the best CPL fit to SMD$(a)^p$ for the two p cases studied here. The assigned colours listed are used consistently in Figs 2-4.

	ω_0	ω_a	plot
DES: BAO+SN+CMB	-0.67±0.10	-1.37±0.50	
DESI: BAO+CMB+Union3	-0.64±0.10	-1.27±0.37	
DESI: BAO+CMB+DESY5	-0.73±0.07	-1.05±0.29	
DESI: BAO+CMB+Pantheon plus	-0.83±0.06	-0.75±0.27	
Best CPL fit to SMD(a) with p=0.606	-0.76	-1.29	
Best CPL fit to SMD(a) with p=0.461	-0.81	-0.99	

 doi:10.20944/preprints202506.2213.v1

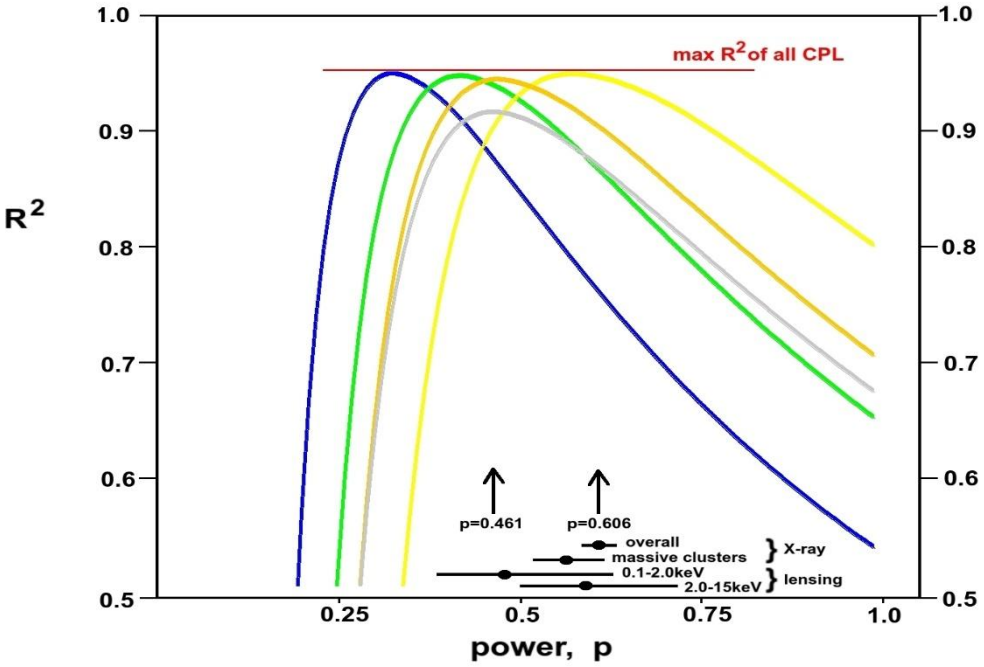

Figure 2. Plot of the variation of the R^2 coefficient of determination against p for each of the three DESI and one DES ω_0 -ω_a CPL values listed in Table 1. The grey curve is the average of all four. The measured p values for galaxies, groups and galaxy clusters shown below is taken from [19].

For all combinations of ω_0 and ω_a values in steps of 0.01, over the wide range +0.9 to -3.0, we found the best fit to SMD(a) measurements (maximum R^2) that are also listed in Table 1 for the two chosen values of p. Both of these ω_0 - ω_a values lie well within the range determined by DESI and DES. These maximum R^2, best fit values are listed in Table 2, together with the R^2 values for the four DES & DESI ω_0 - ω_a values. The DES R^2 values at p=0.606 and the DESI/Union3 at p=0.641 are high at 0.947, close to the maximum of 0.953 of all ω_0 - ω_a space for fits to this survey of SMD(a) measurements.

Table 2. Assuming an IDE source of dark energy and with temperature proportional to (mass)^p, the coefficients of determination, R^2, show how well the ω_0 - ω_a values of Table 1 fit the survey of SMD(a) measurements.

	R^2	
	p=0.606	p=0.461
IDE: best CPL fit (highest R^2)	0.953	0.953
DES: BAO+SN+CMB	0.947	0.912
DESI: BAO+CMB+Union3	0.904	0.947
DESI: BAO+CMB+DESY5	0.866	0.94

 doi:10.20944/preprints202506.2213.v1

DESI: BAO+CMB+Pantheon plus	0.76	0.874

In Figure 3 we further illustrate the similarity between star/structure formation and dark energy histories. For each of the two selected values of p we provide 2 plots. The right-hand plot shows the four DESI and DES 68% and 95% likelihood plots as a function of ω_0 and ω_a . Superimposed are the >0.90 and >0.94 R^2 contours of IDE over all ω_0–ω_a space derived solely from the survey of measured SMD(a). The location of centre points of DESI and DES plots (listed in Table 1) are highlighted together with the point of maximum R^2 of the IDE plot. The left-hand plots illustrate how well the curves corresponding to those highlighted ω_0 - ω_a values fit the survey of stellar mass density measurements.

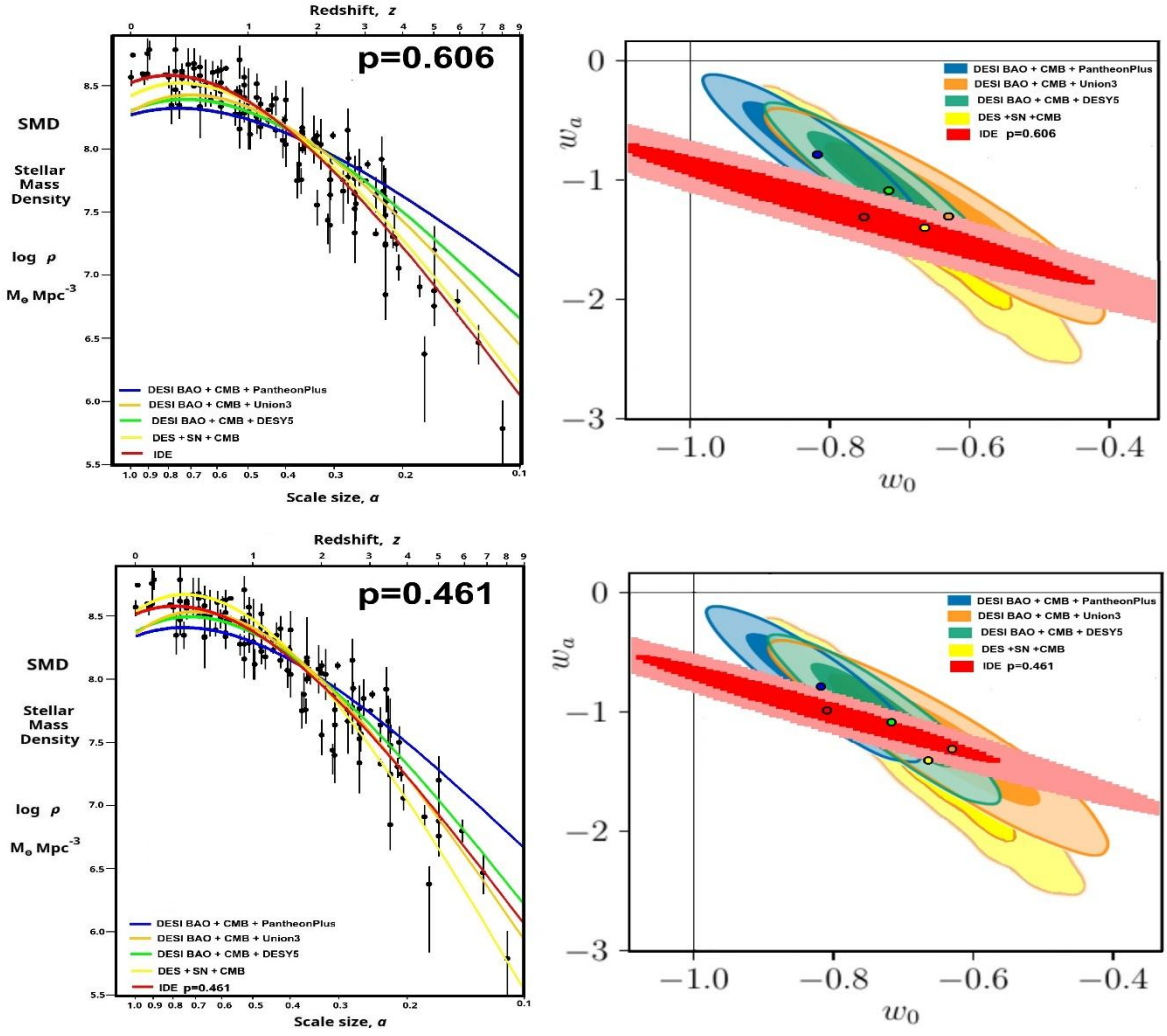

Figure 3. Predicted IDE ω_0-ω_a space contours for $R^2 > 0.90$ and $R^2 > 0.94$ are compared against the measured dark energy 68% and 95% likelihood contours of DESI and DES on the right-hand side. The coloured circles indicate the relevant ω_0 - ω_a peak locations, and used to define the relevant curves on the left-hand side for comparison against the survey of stellar mass density measurements [20-49]. Upper plots are for p=0.606 and lower plots are for p=0.461.

 doi:10.20944/preprints202506.2213.v1

3. Discussion

It is clear from Figure 3 (Left-hand plots) and from the R^2 values in Table2 that the DES most constrained result and the DESI BAO+CMB+Union 3 result both make a good fit to the SMD(a) measurement survey with curves closely following the highest R^2 red curve. Moreover, the range in $\omega_0 - \omega_a$ space that fits SMD(a) measurements with $R^2 > 0.94$ makes a good fit to the DESI and DES dark energy measurements (Figure 3. Right-hand plots). This suggests that the dark energy history is directly related to the history of astrophysical structure temperature and formation, as we expect for an IDE source.

Figure 4 provides an interpretation of predicted IDE and DES & DESI measurements.

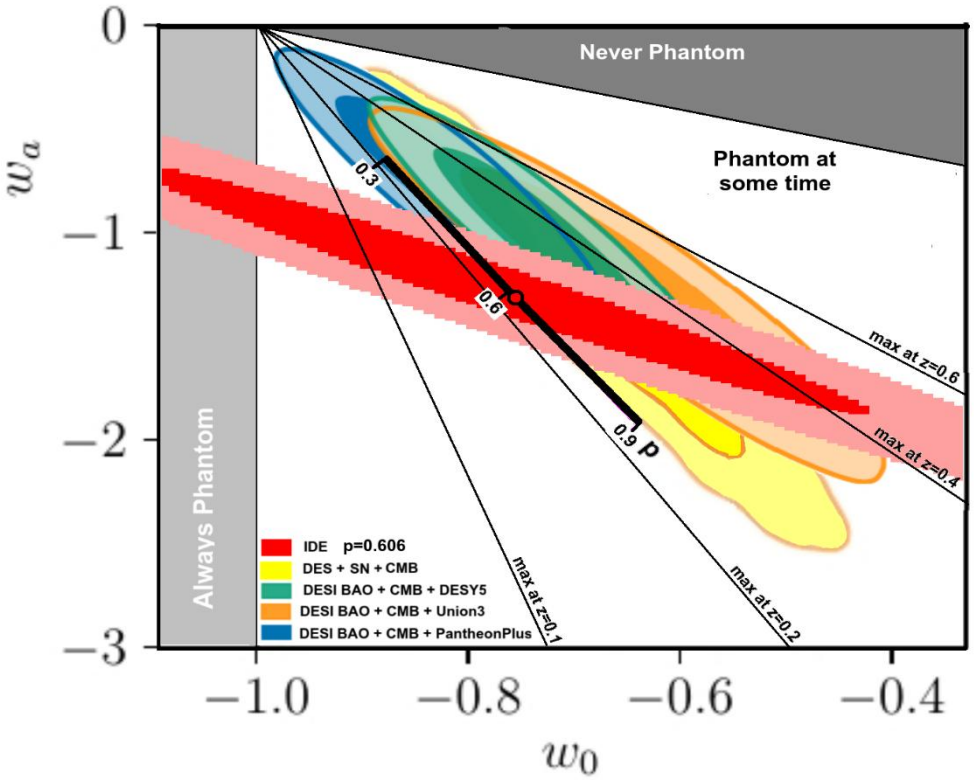

Figure 4. Interpretation of the predicted IDE result with the dark energy measurements of DESI and DES as a phantom dark energy that reached a maximum in the range $0.2<z<0.6$. The thick black line indicates how the IDE peak and contours move with different values of p.

Both the IDE prediction and DESI/DES measurements are consistent with a dark energy that was phantom (increasing energy density) throughout the majority of universe history but is now starting to decrease after recently reaching a maximum. The IDE prediction and DESI/DES measurements are also both consistent with a maximum located in the range $0.2 < z < 0.6$.

Figure 3 (right-hand side) illustrates a difference of IDE contours in ω_0 - ω_a space between the two selected values of p. Figure 4 (thick black line) further illustrates this by showing how the maximum R^2 point moves over a wider range of p values.

While the use of CPL parameters has facilitated comparisons between different experiments, and between experiments and theory, there is no reason to expect that the actual dark energy can be fully described by any particular CPL ω_0 - ω_a combination. It is worth noting the following caveat regarding its use. The relevant curves in Figure 3. (left-hand side plots) emphasize how small the decrease is since the maximum. The curves considered in Figure 3. make a good fit to the majority of data, located beyond the maximum. But we note that much closer to z=0 these CPL curves mostly lie below the SMD data points. Furthermore, other surveys of SMD measurements do not show a distinct

 doi:10.20944/preprints202506.2213.v1

peak at low z [51-53]. As the star formation rate has fallen rapidly in recent times, SMD ceases to increase and has lead to a near-constant value at very low redshifts. If the same effect applies to the dark energy measurements, then the highest dark energy density to date might be occurring now at z=0. Then the perceived recent peak in dark energy density at 0.2<z<0.6 might be just an illusion created by the best CPL parameter fit being primarily determined by higher z data.

The expanding universe has lead to overall matter and radiation energy densities naturally falling as a^{-3} and a^{-4} respectively. In contrast, the stellar mass density and the dark energy density have both increased over time, in a way that is consistent with IDE being the dark energy source driven by star and structure formation. This work emphasizes simplicity, wielding Occam's razor, and naturalness, relying on mostly proven physics, with a strong dependence on data. The potential of IDE to solve problems of cosmology has been covered before (see [16]) and is listed briefly again here for completeness and summarised in Table 3:

1. Information/entropy estimates show that IDE can account for the value of the present dark energy density (see Figure 7 of [16]).
2. Figs 2-4 show that the history of IDE is consistent with the latest DESI and DES $\omega_0 - \omega_a$ results describing the history of dark energy.
3. As IDE fits the latest $\omega_0 - \omega_a$ experiment data much better than Λ, then the Cosmological Constant problem could be resolved by assuming Λ=0, a more likely value [54].
4. As the maximum star formation has only occurred recently (now?), this is the most likely time for intelligent beings to have evolved to live in the dark energy dominated epoch, effectively resolving the "Why now?" Cosmological Coincidence problem.
5. The primarily phantom time history of IDE is similar to several dark energy histories [55-57] that have been shown capable of resolving both H_0 and σ_8 tensions.
6. As the information energy of matter is clumped in astrophysical structures at a similar energy density to matter, IDE may account for some dark matter attributed effects.
7. The location of baryons in galaxies has been shown to fully specify the location of dark matter attributed effects [58,59] as to be expected if IDE accounts for such effects.

Table 3. Potential of IDE to resolve many problems of cosmology. Comparison of IDE against ΛCDM, scalar fields/ quintessence, & MOND.

	Required dark side property	IDE	ΛCDM	Scalar fields/ Quintessence	MOND
1	Account for present dark energy density	YES, order of magnitude, ~10^{70} J	NO, not by many orders	Only by much fine tuning	----
2	Consistent with $\omega_0 - \omega_a$ experiment data	YES, good agreement	NO, >3σ disagreement	Not specific **-1<ω<+1**	----
3	Resolve Cosmological constant problem	YES, $\Lambda \rightarrow 0$	NO	Only by much fine tuning	----
4	Resolve Cosmological coincidence problem	YES, naturally	NO	Only by much fine tuning	----
5	Resolve H_0 and σ_8 tensions	YES, probably	NO	NO	----
6	Account for size of dark matter attributed effects	YES, order of magnitude	NO, DM not detected yet	----	YES, sometimes
7	Account for location of DM attributed effects	YES, coincident with baryons	NO, not coincident	----	YES, coincident with baryons

 doi:10.20944/preprints202506.2213.v1

4. Summary

The approach taken here has been primarily driven by data and indicates a strong similarity between stellar mass density and dark energy histories. We have shown that IDE predicts a dark energy history that matches the dark energy measurements of DESI and DES with a clear overlap in $\omega_0 - \omega_a$ space. Equally, the SDM(a) variation required for an IDE source of dark energy to provide the experimentally measured dark energy $\omega_0 - \omega_a$ combinations matches the measured SDM(a) measurements. The fit between IDE prediction and the latest DES and DESI results, combined with IDE's ability to resolve many dark side problems and tensions, suggests IDE should be considered a strong candidate for the source of observed dark energy.

Funding: This research received no external funding.

Institutional Review Board Statement: Not applicable.

Data Availability Statement: Data available in a publicly accessible repository.

Acknowledgments: This work was enabled by the award of Emeritus Professor of Space Science from the University of Sussex.

Conflicts of Interest: The author declares no conflicts of interest.

References

1. Landauer,R., Irreversibility and heat generation in the computing process, IBM J. Research and Development 1961, 3, 183-191. https://doi.org/10.1147/rd.53.0183
2. Landauer, R., Information is physical, Physics Today, 1991, 44 , 23-29. https://doi.org/10.1063/1.881299
3. Toyabe, S., Sagawa, T., Ueda,M., Muneyuki,E., Sano,M., Experimental demonstration of information-to-energy conversion and validation of the generalized Jarzynski equality, Nature Physics, 2010, 6, 988-992. https://doi.org/10.1038/nphys1821
4. Berut, A., Arakelyan,A., Petrosyan, A., Ciliberto,A., Dillenschneider, R., Lutz,E., Experimental verification of Landauer's principle linking information and thermodynamics, Nature , 2012, 483, 187-189. https://doi.org/10.1038/nature10872
5. Jun,Y., Gavrilov,M., Bechhoefer, J.,High-PrecisionTest of Landauer's Principle in a Feedback Trap, Phys.Rev. Let. 2014, 113, 190601-1 to -5. https://doi.org/10.1103/PhysRevLett.113.190601
6. Yan, L.I.,et al., Single Atom Demonstration of the Quantum Landauer Principle, Phys.Rev. Let. 2018, 120, 210601. https://doi.org/10.1103/PhysRevLett.120.210601
7. Leff,H.S. and Rex,A.F., Maxwell's Demon 2, Institute of Physics Publishing, 1990, ISBN 0-7503-0759-5
8. Zeilinger,A., A Foundational Principle of Quantum Mechanics, Foundations of Physics, 1999, 29, 631-643. http://doi.org/10.1023/A:1018820410908
9. Gough,M.P., Carozzi, T., Buckley,A.M., On the similarity of Information Energy to Dark Energy, Physics Essays, 2006, 19, 446-450. https://doi.org/10.4006/1.3025815
10. Peebles,P.J.E., Principles of Physical Cosmology, 1993, Princeton University Press,Princeton NJ, USA. ISBN 978-0691209814.
11. Gough,M.P., Information Equation of State, Entropy, 2008,10, 150-159. https://doi.org/10.3390/entropy-e10030150
12. Gough,M.P., Holographic Dark Information Energy, Entropy, 2011, 13 , 924-035. https://doi.org/10.3390/e13040924
13. Gough,M.P., Holographic Dark Information Energy: Predicted Dark Energy Measurement, Entropy, 2013, 15, 1133-1149. https://doi.org/10.3390/e15031135
14. Gough,M.P., A Dynamic Dark Information Energy Consistent with Planck Data, Entropy, 2014, 16, 1902-1916. https://doi.org/10.3390/e16041902
15. Gough,M.P., Information Dark Energy can Resolve the Hubble Tension and is Falsifiable by Experiment, Entropy, 2022, 24, 385-399. https://doi.org/10.3390/e24030385
16. Gough, M.P., Evidence for a dark energy driven by star formation: Information Dark Energy, Entropy, 2025, 27,110, https://doi.org/10.3390/e27020110

 doi:10.20944/preprints202506.2213.v1

17. DESI Collaboration, DESI 2024 VI: cosmological constraints from the measurements of baryon acoustic oscillations, Journal of Cosmology and Astroparticle Physics, 2025/02/21. https://doi.org/10.1088/1475-7516/2025/02/021
18. DES CollaboArration, Dark Energy Survey: implications for cosmological expansion models from the final DES Baryon Acoustic Oscillation and Supernova data, arXiv: 2503.06712v1, 9th March, 2025. https://doi.org/10.48550/arXiv.2503.06712
19. Babyk,I.V., McNamara,B.R., The Halo Mass-Temperature Relation for Clusters, Groups, and Galaxies, Astrophysical Journal, 2023, 946, 54. https://doi.org/10.3847/1538-4357/acbf4b
20. Li,C., White, S.D.M., The distribution of stellar mass in the low-redshift universe, Mon. Not. R. Astron. Soc. , 2009, 398 , 2177-2187. https://doi.org/10.1111/j.1365-2966.2009.15268.x
21. Gallazzi,A., Brinchmann, J., Charlot, S., White, S.D.M., A census of metals and baryons in stars in the local universe, Mon. Not. R. Astron. Soc. 2008, 383, 1439-1458. https://doi.org/10.1111/j.1365-2966.2007.12632.x
22. Moustakas,J., et al., PRIMUS: constraints on star formation quenching and Galaxy merging and the evolution of the stellar mass function from z=0-1, Astrophys. J. , 2013, 767, 50. 34pp. https://doi.org/10.1088/0004-637X/767/1/50
23. Bielby,R., et al., The WIRCam Deep Survey. I. Counts, colours, and mass functions derived from near-infrared imaging in the CFHTLS deep fields, Astron. Astrophys. 2012, 545, A23. 20pp. https://doi.org/10.1051/0004-6361/201118547
24. Perez-Gonzalez,P.G., et al., The stellar mass assembly of galaxies from z=0-4: analysis of a sample selected in the rest-frame near infrared with Spitzer, Astrophys. J.,2008, 675, 234-261. https://doi.org/10.1086/523690
25. Ilbert,O., et al., Mass assembly in quiescent and star-forming Galaxies since z >4 from UltraVISTA, Astron.Astrophys. 2013, 556, A55. 19pp https://doi.org/10.1051/0004-6361/201321100
26. Muzzin,A., et al., The evolution of the stellar mass functions of star-forming and quiescent galaxies to z=4 from the COSMOS/UltraVISTA survey, Astrophys. J. , 2013, 777 , 18. 30pp https://doi.org/10.1088/0004-637X/777/1/18
27. Arnouts,S., et al., The SWIRE-VVDS-CFHTLS surveys: Stellar Assembly over the last 10Gyr Astron.Astrophys. 2007, 476, 137-150. https://doi.org/10.1051/0004-6361:20077632
28. Pozzetti,L., et al., zCOSMOS -10k bright spectroscopic sample. The bimodality in the galaxy stellar mass function, Astron. Astrophys. 2010, 523, A13. 23pp https://doi.org/10.1051/0004-6361/200913020
29. Kajisawa,M., et al., MOIRCS deep survey IV evolution of galaxy stellar mass function back to z 3, Astrophys. J. 2009, 702, 1393-1412. https://doi.org/10.1088/0004-637X/702/2/1393
30. Marchesini,D., van Dokkum, P.G., Forster Schreiber,N.M., Franx, M., Labbe, I., Wuyts, S., The evolution of the stellar mass function of galaxies from z=4 and the first comprehensive analysis of its uncertainties, Astrophys. J. 2009, 701, 1765-1769. https://doi.org/10.1088/0004-637X/701/2/1765
31. Reddy,N.A., et al., GOODS-HERSCHEL measurements of the dust attenuation of typical star forming galaxies at high redshift, Astrophys. J. 2012, 744 , 154. 17pp. https://doi.org/10.1088/0004-637X/744/2/154
32. Caputi, K.J., Cirasuolo, M., Jdunlop,J.S., McLure, R.J., Farrah,D., Almaini, O.,The stellar mass function of the most massive Galaxies at 3<z<5 in the UKIDSS Ultra Deep Survey, Mon. Not. R. Astron. Soc. 2011, 413 , 162-176. https://doi.org/10.1111/j.1365-2966.2010.18118.x
33. Gonzalez, V., Labbe,I., Bouwens, R.J., Illingworth,G., Frank,M., Kriek M., Evolution of galaxy stellar mass functions, mass densities, and mass-to light ratios from z 7 to z 4, Astrophys. J. 2011, 735, L34. 6pp https://doi.org/10.1088/2041-8205/735/2/L34
34. Lee ,K.S., et al., How do star-forming galaxies at z>3 assemble their masses?, Astrophys. J. 2012, 752, 66, 21pp. https://doi.org/10.1088/0004-637X/752/1/66
35. Cole,S., al., The 2dF galaxy redshift survey, Mon. Not. R. Astron. Soc. 2001, 326, 255-273. https://doi.org/10.1046/j.1365-8711.2001.04591.x
36. Dickinson,M., Papovich,C., Ferguson, H.C., Budavari,T., The evolution of the global stellar mass density a 0 < z < 3, Astrophys. J. 2003, 587, 25-40. https://doi.org/10.1086/368111
37. Rudnick,G., et al., The rest-frame optical luminosity density, colour, and stellar mass density of the universe from z = 0 to z = 3., Astrophys. J. 2003, 599, 847-864. https://doi.org/10.1086/379628

38. Brinchmann,J., Ellis, R.S.,The ma.ss assembly and star formation characteristics of field galaxies of known morphology, Astrophys. J. 2000, 536 , L77-L80 https://doi.org/10.1086/312738
39. Elsner,F., Feulner,G., Hopp, U.,The impact of Spitzer infrared data on stellar mass estimates, Astron. Astrophys. 2008, 477, 503 -512. https://doi.org/10.1051/0004-6361:20078343
40. Drory,N., Salvato,M., Gabasch,A., Bender, R., Hopp, U., Feuler,G., Pannella, M.,The stellar mass function of galxies to z 5, Astrophys. J. 2005, 619, L131-L134. https://doi.org/10.1086/428044
41. Drory, N., Alvarez,M., The contribution of star formation and merging to stellar mass buildup in galaxies, Astrophys.J. 2008, 680, 41-53. https://doi.org/10.1086/588006
42. Fontana,A., et al., The assembly of massive galaxies from near Infrared observations of Hubble deep-field south, Astrophys. J.2003, 594, L9-L12. https://doi.org/10.1086/378489
43. Fontana,A., et al., The galaxy mass function up to z=4 in the GOODS-MUSIC sample, Astron. Astrophys. 2006, 459, 745-757. https://doi.org/10.1051/0004-6361:20065475
44. Cohen, J.G., CALTECH faint galaxy redshift survey, Astrophys. J. 2002, 567, 672-701. https://doi.org/10.1086/338226
45. Conselice, C.J., Blackburne,J.A., Papovich,C., The luminosity, stellar mass, and number density evolution of field galaxies, Astrophys. J. 2005, 620, 564-583. https://doi.org/10.1086/426102
46. Borch,A., et al., The stellar masses of 25000 galaxies at 0.2<z < 1.0 estimated by COMBO-17 survey, Astron. Astrophys. 2006, 453, 869-881. https://doi.org/10.1051/0004-6361:20054376
47. Madau, P., Dickinson, M., Cosmic Star Formation History, Ann. Rev. Astron. Astrophys. 2014, 52, 415-486.
48. https://doi.org/10.1146/annurev-astro-081811-125615
49. Yabe, K.; Ohta, K.; Iwata, I.; Sawicki, M.; Tamura, N.; Akiyama, M.; Aoki, K. The stellar populations of Lyman break galaxies at z~5. Astrophys. J. 2009, 693, 507 https://doi.org/10.1088/0004-637X/693/1/507
50. Labbe, I.; Oesch, P.A.; Bouwens, R.J.; Illingworth, G.D.; Magee, D.; Gonzalez, V.; Carollo, C.M.; Franx, M.; Trenti, M.; van Dokkkum, P.G.; et al. The spectral energy distributions of z = 8 galaxies from the IRAC ultra deep fields. Astrophys. J. 2013, 777, L19. https://doi.org/10.1088/2041-8205/777/2/L19
51. Chevallier,M., Polarski, D., Accelerating universes with scaling dark matter, Int. J. Mod. Phys. 2001, D. 10 , 213-224. https://doi.org/10.1142/S0218271801000822
52. Wilkins S. M., Trentham N., Hopkins A. M., The evolution of stellar mass and the implied star formation history. MNRAS, 2008, 385, 687. https://doi.org/10.1111/j.1365-2966.2008.12885.x
53. Driver S.P., et al., GAMA/G10-COSMOS/3D-HST: the 0 < z < 5 cosmic star formation history, stellar-mass, and dust-mass densities. MNRAS, 2018, 475, 2891 (D18). https://doi.org/10.1093/mnras/stx2728
54. Koushan, S., Driver, S.P., et al., GAMA/DEVILS: constraining the cosmic star formation history from improved measurements of the 0.3–2.2 μ m extragalactic background light, MNRAS, 2021, 503, 2033-2052. https://doi.org/10.1093/mnras/stab540
55. Weinberg, S.,The cosmological constant problem, Rev. Mod. Phys. 1989, 61, 1-23. https://doi.org/10.1103/RevModPhys.61.1
56. Benevento,G., Hu,W., Raven,M., Can late dark energy raise the Hubble constant?, Phys. Rev. D, 2020, 101, 103517-1-7, https://doi.org/10.1103/PhysRevD.101.103517
57. Keeley,R., Joudaki,S., Kaplinghat, M., Kirkby,D., Implications of a transition in the dark energy equation of state for the H0 and σ8 tensions, J. Cosmol. Astropart. Phys. 2019, 12, 035. https://doi.org/10.1088/1475-7516/2019/12/035
58. Peracaula,J.S., Gomez-Valent,A., De Cruz Perez,J., Moreno-Pulido,C., Running vacuum against the H0 and σ8 tensions, Exploring the Frontiers of Physics, 2021, 134, 19001. p1-p7. https://doi.org/10.1209/0295-5075/134/19001
59. McGaugh, S.S., Lelli,F., Schombert, J.M.,The Radial Acceleration Relation in Rotationally Supported Galaxies, Phys. Rev. Lett. 2016, 117, 201101-1 to -6. https://doi.org/10.1103/PhysRevLett.117.201101
60. Lelli,F., McGaugh,S.S., Schombert, J.M., Pawlowski, M.S.,One Law to Rule them all: the Radial Acceleration relation of Galaxies, Astrophys. J. , 2017, 836, 152. 23pp. https://doi.org/10.3847/1538-4357/836/2/152

 doi:10.20944/preprints202506.2213.v1

disclaim responsibility for any injury to people or property resulting from any ideas, methods, instructions or products referred to in the content.